BIOCHEMISTRY
including biophysical chemistry & molecular biology

Article

pubs.acs.org/biochemistry

Roles of Amino Acids in the *Escherichia coli* Octaprenyl Diphosphate Synthase Active Site Probed by Structure-Guided Site-Directed Mutagenesis

Keng-Ming Chang,[†] Shih-Hsun Chen,[∥] Chih-Jung Kuo,[†,‡] Chi-Kang Chang,[§] Rey-Ting Guo,[†,‡] Jinn-Moon Yang,[∥] and Po-Huang Liang*[,†,‡,§]

[†]Institute of Biochemical Sciences, National Taiwan University, Taipei 106, Taiwan

[‡]Taiwan International Graduate Program, Academia Sinica, Taipei 115, Taiwan

[§]Institute of Biological Chemistry, Academia Sinica, Taipei 115, Taiwan

[∥]Department of Biological Science and Technology, National Chiao Tung University, Hsin-Chu 300, Taiwan

Supporting Information

ABSTRACT: Octaprenyl diphosphate synthase (OPPS) catalyzes consecutive condensation reactions of farnesyl diphosphate (FPP) with five molecules of isopentenyl diphosphates (IPP) to generate C_{40} octaprenyl diphosphate, which constitutes the side chain of ubiquinone or menaquinone. To understand the roles of active site amino acids in substrate binding and catalysis, we conducted site-directed mutagenesis studies with *Escherichia coli* OPPS. In conclusion, D85 is the most important residue in the first DDXXD motif for both FPP and IPP binding through an H-bond network involving R93 and R94, respectively, whereas R94, K45, R48, and H77 are responsible for IPP binding by providing H-bonds and ionic interactions. K170 and T171 may stabilize the farnesyl carbocation intermediate to facilitate the reaction, whereas R93 and K225 may stabilize the catalytic base ($MgPP_i$) for H_R proton abstraction after IPP condensation. K225 and K235 in a flexible loop may interact with FPP when the enzyme becomes a closed conformation, which is therefore crucial for catalysis. Q208 is near the hydrophobic part of IPP and is important for IPP binding and catalysis.

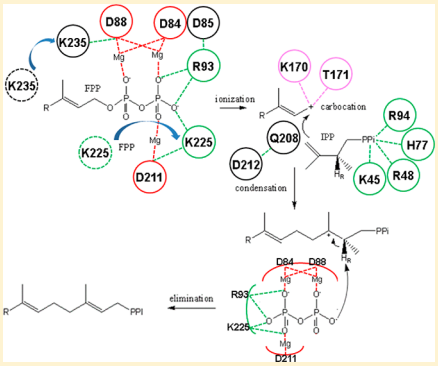

A group of prenyltransferases catalyze consecutive condensation reactions of designated numbers of C_5 isopentenyl diphosphate (IPP) with C_{15} farnesyl diphosphate (FPP) to generate linear isoprenoid natural products.[1−3] On the basis of the stereochemistry of double bonds formed in the IPP condensation reactions, these enzymes are classified as *trans* or *cis* types.[4] FPP is synthesized by FPP synthase (FPPS), also a *trans*-prenyltransferase, through the condensation of two IPPs with its allylic isomer, dimethylallyl diphosphate (DMAPP).[5,6] From FPP, the *trans*-prenyltransferases synthesize C_{20} geranylgeranyl diphosphate as a precursor of many natural products (e.g., Taxol) and as used for protein post-translational modification, C_{25} farnesylgeranyl diphosphate to form ether-linked lipids in thermophilic archaea, and C_{30}−C_{50} products that constitute side chains of ubiquinone and menaquinone.[7,8]

A key feature for *trans*-prenyltransferases is that they all possess two Asp-rich DDXXD motifs. Previous site-directed mutagenesis studies reported that all Asp residues in these motifs of FPPS except the last one in the second motif are important for both substrate binding and catalysis before detailed structural information was available.[9−13] However, as indicated by our crystal structures of *Thermotoga maritima* octaprenyl diphosphate synthase (OPPS) that catalyzes the consecutive condensation reactions of FPP with five IPPs leading to a C_{40} product, two sulfate ions, S1 and S2, which mimic the pyrophosphate group of the substrates, are bound in the active site; S1 is bound with a Mg^{2+} coordinated by the first DDXXD motif, but surprisingly, S2 is held by a positively charged pocket formed by Lys, His, and Arg residues, rather than the conserved DDXXD motifs.[14] By aligning with the more recently published ternary complex structures of FPPS with an inactive DMAPP thiol analogue (DMSPP) and IPP,[15] S1 and S2 sites are presumably for FPP and IPP binding, respectively. Since then, a site-directed mutagenesis study has not been performed in FPPS, OPPS, or any other *trans*-prenyltranferase to verify the exact catalytic roles and the importance of the active site residues. There is no available structure for *trans*-prenyltransferase with bound FPP or IPP.

In the previous study, we utilized a bromo-substituted IPP analogue (Br-IPP) to slow the IPP condensation step and successfully trapped the farnesyl carbocation intermediate as farnesol (FOH) with a base in the *Escherichia coli* OPPS

Received: January 17, 2012
Revised: April 3, 2012
Published: April 3, 2012

reaction.[16] This result further strengthened the ionization−condensation−elimination sequential mechanism previously proposed for FPPS reaction,[17] where the allylic substrate (DMAPP in FPPS and FPP in OPPS) releases pyrophosphate to form the carbocation intermediate, which is attacked by IPP to form the second carbocation intermediate, followed by abstraction of the H_R proton on the IPP moiety to generate the C_5-extended product. On the basis of this reaction mechanism, we examined the possible catalytic roles of the potential active site amino acids by performing site-directed mutagenesis on *E. coli* OPPS using its structure derived by homology modeling from the available *T. maritima* OPPS structure[14] and comparing that structure with the *E. coli* FPPS complex structure.[15] Our results clarify or reveal the roles of previously proposed or unidentified important amino acids and enhance our understanding of the catalytic mechanism of *trans*-prenyltransferases.

Table 1. Primers Used To Construct *E. coli* Mutant OPPS

mutant	primer sequence[a]
D84A	5′-GCTACACGCCGACGTTGT-3′
D85A	5′-ACGACGCCGTTGTGGAT-3′
D88A	5′-GACGTTGTGGCAGAATCAGAT-3′
R93A	5′-CAGATATGGCCAGGGGTAAA-3′
R94A	5′-ATATGCGCGCGGTAAAG-3′
K45A	5′-CGGTGCACGTATTCGTCC-3′
R48A	5′-GTAAACGTATTGCTCCGATGATT-3′
H77A	5′-AGTTTATCGCCACGGCGA-3′
D211A	5′-TTGATCGCCGATTTACTCG-3′
D212A	5′-TGATCGACGCATTACTCGAT-3′
D215A	5′-GATTTACTCGCCTACAATGCC-3′
K170L	5′-ATCTACAGCCTGACTGCGC-3′
K225L	5′-AACAGTTAGGTCTAAACGTCGG-3′
K235L	5′-AAGGTTTACCGACGCTGC-3′
T171V	5′-ATCTACAGCAAGGTTGCGC-3′
Q208A	5′-GCTTTCGCGTTGATCGAC-3′

[a]The mutagenic nucleotides are underlined.

EXPERIMENTAL PROCEDURES

Materials. Radiolabeled [^{14}C]IPP (55 μCi/mmol) and [^{3}H]FPP (17 Ci/mmol) were purchased from Amersham Pharmacia Biotech., and FPP was obtained from Sigma. *PfuTurbo* DNA polymerase was obtained from Life Technologies, Inc. The plasmid mini-prep kit, the DNA gel extraction kit, and NiNTA resin were purchased from Qiagen. The protein expression kit, including the pET16b and pET32Xa/LIC vectors, and competent JM109 and BL21(DE3) cells were obtained from Novagen. The QuikChange site-directed mutagenesis kit was obtained from Stratagene. All commercial buffers and reagents used are of the highest grade.

Homology Modeling of the *E. coli* OPPS Structure. The sequence homology between *E. coli* and *T. maritima* OPPS was calculated with CLUSTAL W multiple-sequence alignment software.[18] On the basis of the sequence homology, the three-dimensional (3D) model of *E. coli* OPPS was generated from the crystal structure (Protein Data Bank entry 1V4E) of *T. maritima* OPPS[14] by using MODELER[19] encoded in Insight II (Accelrys, Inc.), which uses a spatial restraint method to build the 3D protein structure. The structure with the lowest violation score and lowest energy was chosen as the candidate. The distribution of the backbone dihedral angles of the model was evaluated by a Ramachandran plot using PROCHECK.[20] The Prostat module of Insight II was used to analyze the properties of bonds, angles, and torsions. Profile-3D[21] was used to check structure and sequence compatibility.

Site-Directed Mutagenesis of *E. coli* OPPS. OPPS mutants were prepared by using the QuikChange site-directed mutagenesis kit on the *E. coli* OPPS-encoding gene cloned in

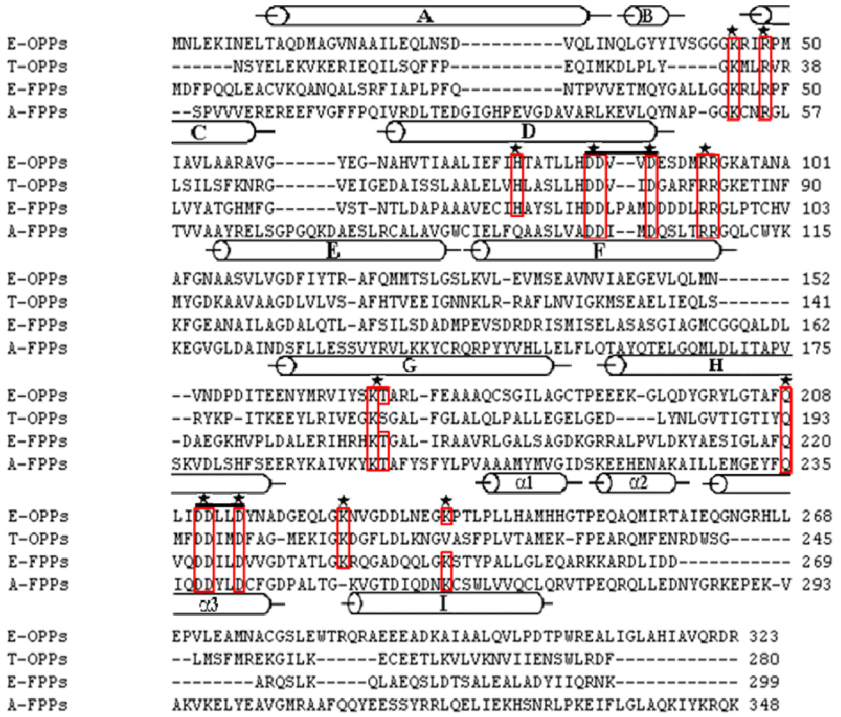

Figure 1. Alignment of amino acid sequences of *E. coli* OPPS (E-OPPs), *T. maritima* OPPS (T-OPPs), *E. coli* FPPS (E-FPPs), and avian FPPS (A-FPPs). The two conserved DDXXD motifs are top-lined. Stars denote the amino acid residues mutated for *E. coli* OPPS in this study.

dx.doi.org/10.1021/bi300069j | *Biochemistry* 2012, 51, 3412−3419

the vector as previously described.[22,23] The mutagenic oligonucleotides prepared by Biobasic Inc. for performing site-directed mutagenesis are listed in Table 1. Each specific amino acid mutation was confirmed by sequencing the entire gene of the cloning plasmid obtained from an overnight culture. The correct construct was subsequently transformed into *E. coli* BL21(DE3) cells for protein expression. The protein purification procedure was described previously.[14] Briefly, the cells were disrupted and purified using NiNTA column chromatography followed by removal of the His tag using FXa. The purified OPPS mutants were checked by SDS−PAGE.

Measurements of Kinetic Parameters for Mutant *E. coli* OPPS. For enzyme activity measurements, each mutant OPPS was used at 0.1 μM. The enzyme reaction was initiated in a 200 μL buffer solution containing 100 mM Hepes (pH 7.5), 5 μM FPP, 50 μM [^{14}C]IPP, 50 mM KCl, and 0.5 mM $MgCl_2$ at 25 °C. The reaction was terminated by addition of 10 mM (final concentration) EDTA, and the product was extracted with 1-butanol. The product was quantitated by counting the radioactivity in the butanol phase ([^{14}C]IPP was in the aqueous phase) using a Beckman LS6500 scintillation counter. The steady-state k_{cat} and K_m values of the mutant enzymes were calculated on the basis of the the initial rates of IPP consumption as previously described.[22,23]

Circular Dichroism (CD) Experiments. CD spectra of wild-type and mutant OPPS were recorded by using a Jasco J-815 spectrophotometer at 25 °C. Measurements of melting temperature (T_m) were performed at 222 nm between 20 and 95 °C (1 °C/min) using 1 mm quartz cells. The protein samples were diluted in 25 mM Tris-HCl (pH 7.5) and 150 mM NaCl buffer to a working concentration of 0.33 mg/mL. T_m values were determined by fitting the curves of CD signal versus temperature using Excel.

Trapping of the Farnesyl Carbocation Intermediate in the Mutant OPPS Reactions. The farnesol that resulted from the farnesyl carbocation intermediate was trapped according to the procedure described previously.[16] To a reaction mixture containing 10 μM wild-type or mutant OPPS, 50 μM Br-IPP, 0.5 mM $MgCl_2$, 50 mM KCl, and 0.1% Triton X-100 in 100 mM Hepes-KOH buffer (pH 7.5) at 25 °C was added 2 μM [^{3}H]FPP to initiate the enzyme reaction. A portion of the reaction solution (33 μL) was withdrawn after 0, 10, 20, 40, and 60 min and mixed with 67 μL of NaOH (0.6 N) to terminate the enzyme reaction. Octane was utilized to extract the [^{3}H]FOH that resulted from the intermediate, if any, which was quantitated by scintillation counting.

RESULTS AND DISCUSSION

Homology Modeling of the *E. coli* OPPS Structure. To explain the site-directed mutagenesis results, we first constructed the structural model of *E. coli* OPPS from the 3D structure of *T. maritima* OPPS based on the sequence homology as shown in Figure 1 (*E. coli* and *T. maritima* OPPS are 28% identical and 56% similar in terms of full-length sequences and 34% identical and 65% similar in the helix C to α2 regions). Literature supports the possibility that a reasonable structural model can be obtained by homology modeling from a related template that is at least 25% identical in sequence.[24,25] The modeled *E. coli* OPPS structure and *T. maritima* OPPS crystal structure are superimposed well with a root-mean-square deviation (rmsd) of 0.89 Å for 396 matched pairs of main chain atoms, except for the five extra short stretches of amino acids from *E. coli* OPPS, of which three are located in the loop regions and the other two in helices A and I, respectively

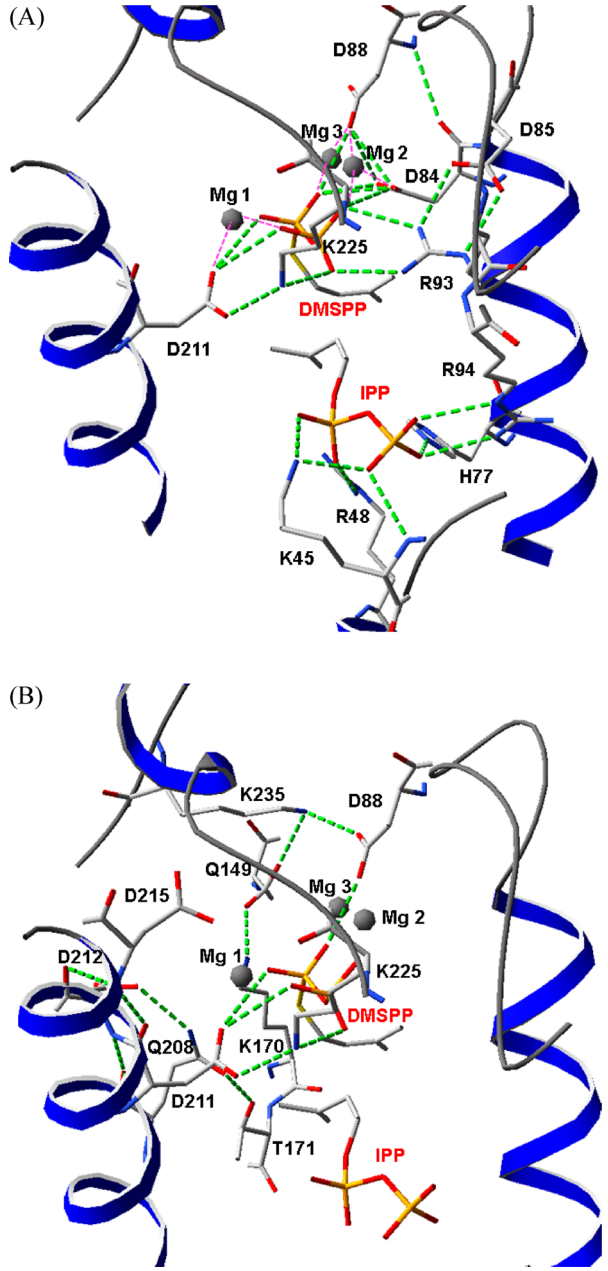

Figure 2. Interactions of the active site amino acids in *E. coli* OPPS with DMSPP and IPP adopted from the FPPS crystal structure. (A) Amino acids binding with DMSPP through Mg^{2+} and ionic interactions and those forming electrostatic or H-bond interactions with IPP. Mg^{2+} ions are shown as gray dots. Oxygens are colored red, nitrogens blue, sulfurs yellow, and carbons white. Hydrogen bonds are represented as green dashed lines. (B) Other amino acids forming H-bonds in the active site.

(see Figure 1A of the Supporting Information). Moreover, amino acids in the active site of *E. coli* OPPS (Figure 1B of the Supporting Information) overlap with those surrounding S1 and S2 in the *T. maritima* OPPS structure. Guided by this model, we performed site-directed mutagenesis studies to test the function of active site amino acid residues as shown below.

Basic Substrate Binding Modes Revealed by the Structural Model. When the modeled *E. coli* OPPS structure is superimposed with the structure of the FPPS−DMSPP−IPP ternary complex (Figure 2A), the pyrophosphate oxygen atoms

dx.doi.org/10.1021/bi300069j | *Biochemistry* 2012, 51, 3412−3419

Table 2. Kinetic Parameters of *E. coli* OPPS Mutants

	FPP K_m (μM)	IPP K_m (μM)	k_{cat} (s^{-1})[e]	x-fold
wild type	1.5 ± 0.4	4 ± 0.3	2 ± 0.1	1
D84A[a]	9.2 ± 1.7	9.3 ± 1.3	(1.2 ± 0.1) × 10^{-4}	6.0 × 10^{-5}
D85A[a]	24.0 ± 4.1	29.4 ± 8.6	(3.2 ± 0.3) × 10^{-4}	1.6 × 10^{-4}
D88A[a]	3.8 ± 0.3	8.5 ± 1.3	(1.1 ± 0.1) × 10^{-4}	5.7 × 10^{-5}
R93A[a]	5.2 ± 1.0	3.7 ± 0.2	(1.2 ± 0.1) × 10^{-4}	5.8 × 10^{-5}
R94A[b]	2.8 ± 0.5	53.9 ± 9.9	(8.4 ± 0.3) × 10^{-5}	4.2 × 10^{-5}
K45A[b]	1.0 ± 0.1	33.5 ± 7.8	(3.6 ± 0.3) × 10^{-3}	1.8 × 10^{-3}
R48A[b]	24.6 ± 1.9	63.9 ± 8.0	(1.1 ± 0.1) × 10^{-3}	5.7 × 10^{-4}
H77A[b]	24.2 ± 6.0	102.6 ± 11.6	(1.9 ± 0.1) × 10^{-2}	9.5 × 10^{-3}
D211A[c]	1.7 ± 0.1	27.1 ± 1.1	(7.5 ± 0.1) × 10^{-3}	3.7 × 10^{-3}
D212A[c]	3.1 ± 0.5	23.3 ± 2.3	(1.8 ± 0.1) × 10^{-3}	9.1 × 10^{-4}
D215A[c]	1.5 ± 0.1	18.2 ± 0.6	(8.7 ± 0.1) × 10^{-3}	4.3 × 10^{-3}
K170L[d]	3.2 ± 0.5	4.9 ± 1.0	(3.3 ± 0.1) × 10^{-4}	1.7 × 10^{-4}
T171V[d]	0.8 ± 0.1	11.3 ± 0.7	(9.1 ± 0.1) × 10^{-3}	4.5 × 10^{-3}
Q208A[d]	1.8 ± 0.2	74.5 ± 8.4	(1.9 ± 0.1) × 10^{-3}	9.6 × 10^{-4}
K225L[d]	1.2 ± 0.1	4.5 ± 1.4	(4.3 ± 0.3) × 10^{-3}	2.2 × 10^{-3}
K235L[d]	0.8 ± 0.1	2.4 ± 0.1	(9.6 ± 0.1) × 10^{-3}	4.8 × 10^{-3}

[a]The amino acids in the S1 site. [b]The amino acids in the S2 site. [c]The amino acids in the second DDXXD motif. [d]The amino acids in the other locations nearby. [e]The value of 2 s^{-1} for wild-type OPPS is the rate of IPP condensation measured under single-turnover conditions,[22] and the k_{cat} values of the mutants were measured under steady-state conditions (see the text).

of the allylic substrate (FPP in OPPS and DMAPP in FPPS) are coordinated by the first DDXXD conserved motif through water−Mg^{2+} chelation. Moreover, two conserved residues, Lys225 and Arg93, are involved in H-bonding interactions with the pyrophosphate of FPP. In addition, the 15-carbon chain of FPP is stretched into the large cavity formed by helices D, F, and G. These interactions place FPP close to IPP with C1 of FPP at a distance suitable for condensation with C4 of IPP.

On the other hand, IPP is bound mainly by the ionic interactions of the positively charged residues such as His77, Arg48, and Lys45 with its pyrophosphate oxygen anions. Moreover, Arg93 and Arg94 are also in the proximity of both FPP and IPP pyrophosphates. The most surprising observation from the structural model is that the pyrophosphate group of IPP is not directly recognized by either Asp-rich motif. This raised the question, to be addressed in this study, of the role of the second DDXXD motif; the first DDXXD motif was expected to be essential for FPP binding via the Mg^{2+} ion cluster as revealed by the structure of the FPPS−DMSPP−IPP complex. Although the pyrophosphate of IPP is surrounded by the positively charged residues at the bottom of helices αD and αE, its hydrophobic carbon tail is stretched toward helices D, G, and H to interact with a number of hydrophobic residues, including Leu81, Thr171, and Phe207.

Preparation of the Mutant OPPS. To address the issue of catalytic roles, we replaced potentially important amino acids in the FPP site, including D84, D85, and D88 in the first DDXXD motif and R93; K45, R48, H77, and R94 in the IPP site; D211, D212, and D215 in the second DDXXD motif; and K170, T171, Q208, K225, and K235 in other locations nearby. The purity of all mutant OPPS was greater than 95% as judged by SDS−PAGE (Figure 2 of the Supporting Information) with a yield of approximately 25 mg/L of culture. The mutant OPPS forms were subjected to steady-state kinetic constant measurements and carbocation intermediate trapping experiments as shown below.

Kinetic Characterization of the Mutant OPPS and the Assigned Roles of the Mutated Amino Acids. As shown in Table 2, the k_{cat} values of the D84A, D85A, and D88A mutants of OPPS were approximately 10^4-fold smaller than the value of 2 s^{-1} for wild-type IPP condensation measured under single-turnover conditions (although the k_{cat} of wild-type OPPS is 0.02 s^{-1}, as limited by product release under steady-state conditions,[22] we have checked here the smaller k_{cat} values of the mutant OPPS are due to the impaired catalysis because product release is not affected by the mutations). Their IPP K_m values were not changed, and FPP K_m values were merely affected by 2−6-fold for the D84A and D88A mutants. However, the D85A mutation not only increased the FPP K_m value by 16-fold but also caused a 7-fold larger IPP K_m value compared to that of the wild type. As shown in Figure 2A, the side chains of D84 and D88 are mainly responsible for coordinating two Mg^{2+} ions (Mg2 and Mg3) for binding with diphosphate oxygens of DMSPP. On the other hand, the side chain of D85 forms H-bonds with R93 that in turn forms an ionic interaction with the DMSPP diphosphate group. This network makes D85 more important in both FPP and IPP binding for OPPS. Similarly, the R93A mutant exhibited a 3-fold slightly increased FPP K_m and a 10^4-fold decreased k_{cat}, but unchanged IPP K_m, indicating its importance for FPP pyrophosphate binding through the ionic interaction and possibly for pyrophosphate release during catalysis. On the other hand, R94 that is adjacent to R93 forms an ionic interaction with the IPP diphosphate from the structural model, and the R94A mutant in fact displayed a 13-fold significantly increased IPP K_m and a 10^{-5}-fold decreased k_{cat} without a change in its FPP K_m.

Substituting K45, R48, and H77 with Ala in the IPP site caused more remarkable increases in IPP K_m values (13-, 16-, and 25-fold, respectively). The K45A, R48A, and H77A mutants also exhibited 10^3-fold smaller k_{cat} values than the wild type (Table 2). As also revealed in Figure 2A, IPP diphosphate is bound with the side chains of K45 and H77 through H-bonds, as well as side chains of R48 and R94 via ionic interactions.

In the second Asp-rich motif, mutants D211A, D212A, and D215A have unchanged FPP K_m values but 4−7-fold increased IPP K_m values and significantly (10^3-fold) reduced k_{cat} values (Table 2), even for D211A, which was expected to have a

dx.doi.org/10.1021/bi300069j | *Biochemistry* 2012, 51, 3412−3419

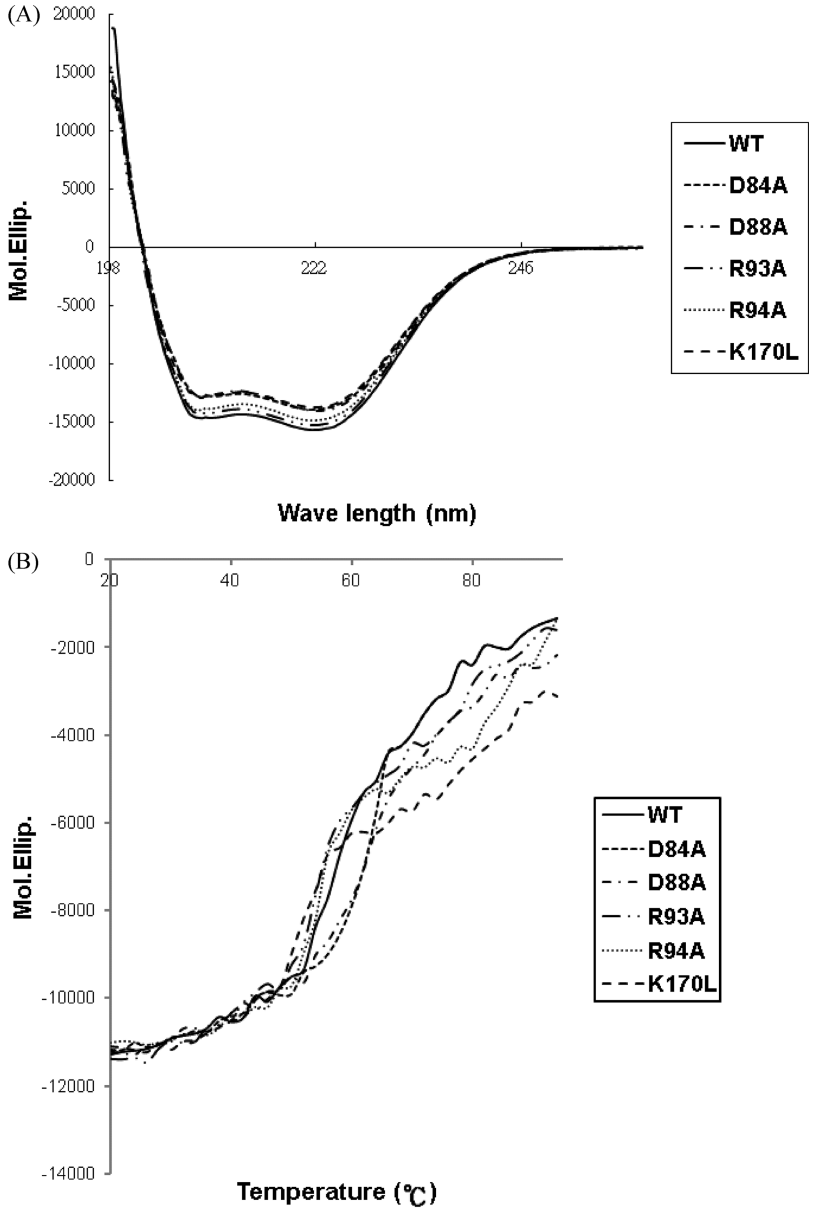

Figure 3. CD spectra of 0.33 mg/mL wild-type OPPS and some of its representative mutants with the most impaired activities. (A) Similar CD spectra of wild-type and mutant OPPS. (B) T_m measurements of wild-type and mutant OPPS using the thermal denaturing CD curves. The data show similar folds and thermostabilities for these enzymes.

greater impact on FPP binding because it coordinates Mg1 according to the structure of the FPPS–DMSPP–IPP complex. The results suggest that Mg1 alone does not play an important role in FPP binding. In contrast, the D211A mutation caused the most increased IPP K_m (Table 2), probably because D211 is close to the carbon moiety of IPP.

In addition to D211, four other amino acids, K170, T171, K225, and Q208, were examined in terms of their roles in substrate binding and catalysis because these residues are also close to DMSPP and IPP in the structural model (Figures 2B). K170L, K225L, and T171V mutations led to 10^3–10^4-fold decreases in k_{cat} values without significantly affecting FPP and IPP K_m values (Table 2). However, replacement of Q208 with Ala led to an unchanged FPP K_m but a significantly (19-fold) increased IPP K_m and a 10^3-fold reduced k_{cat} (Table 2). Although K170 and K225 make direct contact with the DMSPP diphosphate according to Figure 2B, removal of their positively charged Nε atoms did not cause an increased FPP K_m, probably because of the compensation by the H-bonding network for FPP diphosphate. However, K225 may have a role in stabilizing the catalytic base ($MgPP_i$) for H_R abstraction as revealed by the FPPS crystal structure in the catalytically active closed form,[15] and thus, its mutation caused a remarkably reduced k_{cat} value. K170 and T171 may stabilize the farnesyl carbocation intermediate through their backbones and side chains, so that their mutations caused remarkably decreased k_{cat} values. This was confirmed by the failure of the trapping intermediate as shown later. Among these mutants, Q208A has the most increased IPP K_m, indicating its importance in IPP binding.

Another Lys residue, K235, when changed to Leu led to a 10^3-fold decreased k_{cat} value. As revealed in the simulated structure, its side chain forms an H-bond with D88 that is directly involved in allylic substrate binding. Moreover, K225 and K235 are located in a flexible loop between α1 and helix H

dx.doi.org/10.1021/bi300069j | *Biochemistry* 2012, 51, 3412–3419

that might undergo a conformational change upon substrate binding as revealed by comparison of the *E. coli* FPPS structure (closed form) and the avian FPPS structure (open form).[15] When the conformational change occurs, the loss of the H-bond interactions between K225 and K235 side chains and the diphosphate of DMSPP and D88, respectively, may be the reason leading to significantly decreased k_{cat} values (Table 2).

Folding of the OPPS Mutants Probed by CD Spectroscopic Measurements. To prove that the OPPS mutants were folded as well as the wild type and that their lower activities as mentioned above were not due to misfolding, we performed CD spectroscopic measurements on them. As shown in Figure 3A, the CD spectra of the OPPS mutants with the most impaired enzyme activities shown as representatives were similar to that of the wild type, indicating unchanged secondary structures. Moreover, the unfolding temperatures (T_m) for wild-type OPPS and its mutants were measured to be around 56−60 °C (Figure 3B), indicating similar thermal stabilities for them. In fact, the D84A and D88A mutants exhibited slightly higher unfolding temperatures than the wild type. Overall, these data show that the amino acid substitutions did not perturb the enzyme structure.

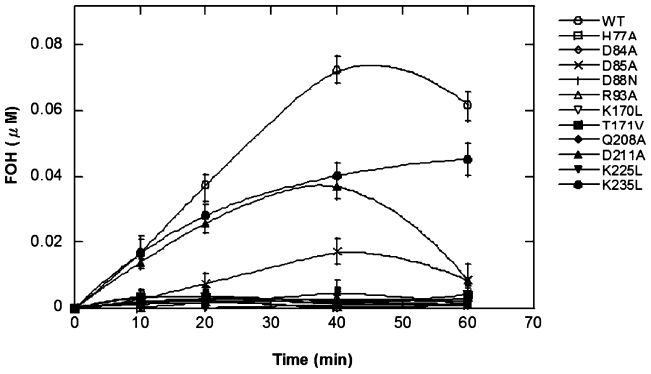

Figure 4. Intermediate trapping for OPPS mutants. The farnesyl carbocation intermediate was trapped in wild-type, Q208A, D211A, and K235L OPPS, but not in other mutant enzymes, when using Br-IPP to slow the condensation step. Results are consistent with the proposed roles of these amino acids (see the text).

Carbocation Intermediate Trapping in the Mutant OPPS. As previously shown, in the presence of an IPP analogue, Br-IPP, the condensation reaction is retarded to allow trapping of the farnesyl carbocation intermediate as FOH in the *E. coli* OPPS reaction.[16] As shown in Figure 4, trapping of the carbocation intermediate in wild-type OPPS served as a positive control. The carbocation intermediates of most OPPS mutants except K235L, D211A, and Q208A were almost not detectable, pointing to the importance of these residues in the initiation of intermediate formation or stabilization of the intermediate. Among them, K235L showed delayed formation of the intermediate, while others showed smaller quantities of intermediate compared to the wild type. With regard to those mutants showing no intermediate, side chain oxygen atoms of T171 and Q208 are oriented with their negative dipoles directed toward the allylic carbocation-binding site as revealed by the FPPS crystal structure.[15] However, as shown in the carbocation trapping experiments, only the T171A mutant failed to yield the intermediate, indicating T171 plays a major role in stabilizing the intermediate by using its side chain OH. Replacement of Q208 with Ala (Q208A) to break the H-bond between its side chain and the side chain hydroxyl group of T171 still maintained some level of intermediate. Furthermore, substitution of K170 with Leu caused the disappearance of the intermediate. This may be due to the fact that the K170 side

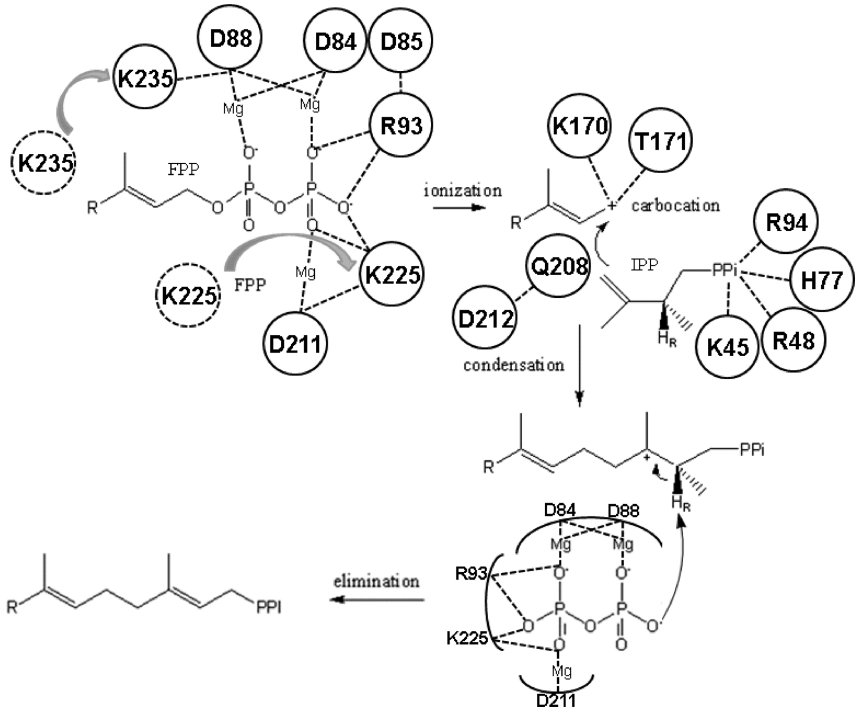

Figure 5. Summary of the roles of important amino acids mutated in this study in catalyzing the OPPS reaction. In the sequential ionization−elimination mechanism, several residues bind with the FPP diphosphate and facilitate its ionization. IPP binding is mainly through ionic interactions. K170 and T171 may stabilize the farnesyl carbocation, and K225 and R93 may stabilize the non-metal-ligated pyrophosphate oxygen as the catalytic base to remove the H_R proton.

dx.doi.org/10.1021/bi300069j | *Biochemistry* 2012, 51, 3412−3419

chain is H-bonded to the side chain of Q149, which is indirectly involved in binding of FPP diphosphate. Amino acids D84, D85, and D88 in the first DDXXD motif and R93 also yielded no intermediate when mutated, consistent with their role in binding with the diphosphate of FPP. K225L failed to maintain the level of the intermediate, although K225 forms only one H-bond with FPP diphosphate in the closed (catalytically active) conformation. Although H77 mainly binds with the diphosphate moiety of IPP, its network interactions with D84, D85, and T80 are apparently important for binding with FPP diphosphate, which is substantiated by the increased FPP K_m value of the H77A mutant and the lack of accumulation of the intermediate.

Conserved Substrate Binding Modes in Other Prenyltransferases. As demonstrated in this study, FPP is bound with the Mg^{2+} ions coordinated mainly by the first DDXXD conserved motif as well as R93 and K225 for ionic interactions, whereas the IPP is mainly bound through the diphosphate moiety with the positively charged K45, H77, R48, and R94 residues in *E. coli* OPPS. This substrate binding mode deduced from the OPPS site-directed mutagenesis study is illustrated in Figure 5. This FPP binding mode of *trans*-prenyltransferases is also found in other enzymes such as squalene synthase,[26] pentalenene synthase,[27] and 5-epi-aristolochene synthase,[28] which utilize FPP as a substrate, with at least one signature Asp-rich sequence for coordinating Mg^{2+}. On the other hand, the IPP binding mode mediated by the positively charged Lys, Arg, and His residues in *trans*-prenyltransferases is shared by that for FPP binding in protein farnesyltransferases and geranylgeranyltransferases.[29,30] Thus, both strategies (through an Asp-rich motif and through ionic interactions) have been observed for the binding of allylic (e.g., FPP) and homoallylic (IPP) substrates in various prenyltransferases, depending on whether Mg^{2+} is required.

CONCLUSION

As shown by the data presented here, we have reached a number of conclusions. (i) In the first DDXXD motif, D85 is the most important residue for substrate binding. (ii) H77 is the most important residue in IPP binding, and R94, but not R93, is important for IPP binding. (iii) The second DDXXD motif, particularly D211, although it coordinates with only one Mg^{2+}, is important for catalysis. (iv) T171 is the main residue for stabilizing the farnesyl carbocation intermediate, whereas R93 and K225 stabilize the catalytic base (Mg^{2+}-diphosphate) for H_R proton abstraction. (v) Q208 forms an H-bond network with T203, D211, and D212 near the IPP binding site, and this H-bond network is important for IPP binding. (vi) K225 and K235 in a flexible loop may interact with FPP and are crucial for catalysis. These conclusions revealed by our site-directed mutagenesis studies based on the simulated and determined structures further enhance our understanding of the roles played by active site amino acid residues and the reaction mechanism of *trans*-prenyltransferases.

ASSOCIATED CONTENT

Supporting Information

Structural model of *E. coli* OPPS and SDS−PAGE of the purified OPPS mutants. This material is available free of charge via the Internet at http://pubs.acs.org.

AUTHOR INFORMATION

Corresponding Author

*Institute of Biological Chemistry, Academia Sinica, 128 Academia Rd., Taipei 115, Taiwan. E-mail: phliang@gate.sinica.edu.tw. Telephone: +886-2-3366-4069. Fax: +886-2-2363-5038.

Author Contributions

K.-M.C. and S.-H.C. made equal contributions to this work.

Funding

This work was supported by grants from Academia Sinica and the National Science Council (Grant 99-2113-M-001-014-MY3).

Notes

The authors declare no competing financial interest.

ABBREVIATIONS

FPP, farnesyl diphosphate; IPP, isopentenyl diphosphate; FPPS, farnesyl diphosphate synthase; DMAPP, dimethylallyl diphosphate; OPPS, octaprenyl diphosphate synthase; DMSPP, dimethylallyl *S*-thiolodiphosphate; Br-IPP, bromo-substituted IPP; FOH, farnesol; Hepes, 4-(2-hydroxyethyl)-1-piperazineethanesulfonic acid; EDTA, ethylenediaminetetraacetic acid; SDS−PAGE, sodium dodecyl sulfate−polyacrylamide gel electrophoresis.

REFERENCES

(1) Kellogg, B. A., and Poulter, C. D. (1997) Chain elongation in the isoprenoid biosynthetic pathway. *Curr. Opin. Chem. Biol. 1*, 570−578.

(2) Ogura, K., and Koyama, T. (1998) Enzymatic aspects of isoprenoid chain elongation. *Chem. Rev. 98*, 1263−1276.

(3) Liang, P. H., Ko, T. P., and Wang, A. H.-J. (2002) Structure, mechanism, and function of prenyltransferases. *Eur. J. Biochem. 269*, 3339−3354.

(4) Liang, P. H. (2009) Reaction Kinetics, Catalytic Mechanisms, Conformational Changes, and Inhibitor Design for Prenyltransferases. *Biochemistry 48*, 6562−6570.

(5) Nishino, T., Ogura, K., and Seto, S. (1972) Substrate specificity of farnesyl pyrophosphate synthetase. *J. Am. Chem. Soc. 94*, 6849−6853.

(6) Ding, V. D., Sheares, B. T., Bergstrom, J. D., Ponpjpom, M. M., Perez, L. B., and Poulter, C. D. (1991) Purification and characterization of recombinant human farnesyl diphosphate synthase expressed in *Escherichia coli*. *Biochem. J. 275*, 61−65.

(7) Poulter, C. D., and Rilling, H. C. (1981) in *Biosynthesis of isoprenoid compounds* (Spurgeon, S. R., Ed.) Vol. *1*, pp 1−282, John Wiley & Sons, New York.

(8) Ogura, K., Koyama, T., and Sagami, H. (1997) in *Subcellular Biochemistry* (Bittman, R., Ed.) Vol. *28*, pp 57−88, Plenum, New York.

(9) Marrero, P. F., Poulter, C. D., and Edwards, P. A. (1992) Effects of site-directed mutagenesis of the highly conserved aspartate residues in domain II of farnesyl diphosphate synthase activity. *J. Biol. Chem. 267*, 21873−21878.

(10) Joly, A., and Edwards, P. A. (1993) Effect of site-directed mutagenesis of conserved aspartate and arginine residues upon farnesyl diphosphate synthase activity. *J. Biol. Chem. 268*, 26983−26989.

(11) Koyama, T., Tajima, M., Sano, H., Doi, T., Koike-Takeshita, A., Obata, S., Nishino, T., and Ogura, K. (1996) Identification of significant residues in the substrate binding site of *Bacillus stearothermophilus* farnesyl diphosphate synthase. *Biochemistry 35*, 9533−9538.

(12) Song, L., and Poulter, C. D. (1994) Yeast farnesyl-diphosphate synthase: Site-directed mutagenesis of residues in highly conserved prenyltransferase domains I and II. *Proc. Natl. Acad. Sci. U.S.A. 91*, 3044−3048.

(13) Koyama, T., Tajima, M., Sano, H., Doi, T., Koike-Takeshita, A., Obata, S., Nishino, T., and Ogura, K. (1996) Identification of significant residues in the substrate binding site of *Bacillus stearothermophilus* farnesyl diphosphate synthase. *Biochemistry 35*, 9533−9538.
(14) Guo, R. T., Kuo, C. J., Chou, C. C., Ko, T. P., Shr, H. L., Liang, P. H., and Wang, A. H.-J. (2004) Crystal structure of octaprenyl pyrophosphate synthase from hyperthermophilic *Thermotoga maritima* and mechanism of product chain length determination. *J. Biol. Chem. 279*, 4903−4912.
(15) Hosfield, D. J., Zhang, Y., Dougan, D. R., Broun, A., Tari, L. W., Swanson, R. V., and Finn, J. (2004) Structural basis for bisphosphonate-mediated inhibition of isoprenoid biosynthesis. *J. Biol. Chem. 279*, 8526−8529.
(16) Lu, Y. P., Liu, H. G., and Liang, P. H. (2009) Different reaction mechanisms for *cis*- and *trans*-prenyltransferases. *Biochem. Biophys. Res. Commun. 379*, 351−355.
(17) Poulter, C. D., Argyle, J. C., and Mash, E. A. (1977) Prenyltransferase. New evidence for an ionization-condensation-elimination mechanism with 2-fluorogeranyl pyrophosphate. *J. Am. Chem. Soc. 99*, 957−959.
(18) Thompson, J. D., Higgins, D. G., and Gibson, T. J. (1994) CLUSTAL W: Improving the sensitivity of progressive multiple sequence alignment through sequence weighting, position-specific gap penalties and weight matrix choice. *Nucleic Acids Res. 22*, 4673−4680.
(19) Sali, A., and Blundell, T. L. (1993) Comparative protein modelling by satisfaction of spatial restraints. *J. Mol. Biol. 234*, 779−815.
(20) Laskowski, R. A., MacArthur, M. W., Moss, D. S., and Thornton, J. M. (1993) PROCHECK: A program to check the stereochemical quality of protein structures. *J. Appl. Crystallogr. 26*, 283−291.
(21) Bowie, J. U., Luthy, R., and Eisenberg, D. (1991) A method to identify protein sequences that fold into a known three-dimensional structure. *Science 253*, 164−170.
(22) Pan, J. J., Kuo, T. H., Chen, Y. K., Yang, L. W., and Liang, P. H. (2002) Insight into the activation mechanism of *Escherichia coli* octaprenyl pyrophosphate synthase derived from pre-steady-state kinetic analysis. *Biochim. Biophys. Acta 1594*, 64−73.
(23) Kuo, T. H., and Liang, P. H. (2002) Reaction kinetic pathway of the recombinant octaprenyl pyrophosphate synthase from *Thermotoga maritima*: How is it different from that of the mesophilic enzyme. *Biochim. Biophys. Acta 1599*, 125−133.
(24) Messaoudi, A., Belguith, H., and Hamida, J. B. (2011) Three dimentional structure of *Arabidopsis thaliana* lipase predicted by homology modeling method. *Evol. Bioinf. Online 7*, 99−105.
(25) Yang, A. S., and Honig, B. (2000) An integrated approach to the analysis and modeling of protein sequences and structures. *J. Mol. Biol. 301*, 665−711.
(26) Pandit, J., Danley, D. E., Schulte, G. K., Mazzalupo, S., Pauly, T. A., Hayward, C. M., Hamanaka, E. S., Thompson, J. F., and Harwood, H. J., Jr. (2000) Crystal structure of human squalene synthase. *J. Biol. Chem. 275*, 30610−30617.
(27) Lesburg, C. A., Zhai, G., Cane, D. E., and Christianson, D. W. (1997) Crystal structure of pentalenene synthase: Mechanistic insights on terpenoid cyclization reactions in biology. *Science 277*, 18200−1824.
(28) Starks, C. M., Back, K., Chappell, J., and Noel, J. P. (1997) Structural basis for cyclic terpene biosynthesis by tobacco 5-epi-aristolochene synthase. *Science 277*, 18150−1820.
(29) Long, S. B., Casey, P. J., and Beese, L. S. (1998) Co-crystal structure of protein farnesyltransferase with a farnesyl diphosphate substrate. *Biochemistry 37*, 96120−9618.
(30) Taylor, J. S., Reid, T. S., Terry, K. L., Casey, P. J., and Beese, L. S. (2003) Structure of mammalian protein geranylgeranyltransferase type-I. *EMBO J. 22*, 59630−5974.